Unusually large polarizabilities and previously unidentified atomic states in Ba

C.-H. Li,[1,*] S. M. Rochester,[1,†] M. G. Kozlov,[2,‡] and D. Budker[1,3,§]
[1]*Department of Physics, University of California at Berkeley, Berkeley, California 94720-7300, USA*
[2]*Petersburg Nuclear Physics Institute, Gatchina 188300, Russia*
[3]*Nuclear Science Division, Lawrence Berkeley National Laboratory, Berkeley, California 94720, USA*
(Received 5 August 2003; revised manuscript received 30 December 2003; published 7 April 2004)

Electric polarizabilities of four even-parity states of atomic barium in the range $35\,600-36\,000\ \mathrm{cm}^{-1}$, excited via two successive $E1$ transitions, are measured using direct spectroscopy. Several states have polarizabilities more than two orders of magnitude larger than might be expected from the known energy levels of Ba, implying the existence of two previously unobserved odd-parity states nearby. These two states are located using Stark-induced excitation, and tentatively identified as $(\mathrm{Xe})6s8p\ ^3P_{0,2}$. The (also unusually high) polarizabilities of these states, as well as that of a third odd-parity state, are reported.

DOI: 10.1103/PhysRevA.69.042507 PACS number(s): 32.10.−f, 32.60.+i

Knowledge of the electric polarizabilities of certain energy levels of barium (not measured in previous studies [1–10]) is useful for the analysis of experiments with Ba searching for violation of Bose-Einstein statistics for photons [11,12]. We have measured scalar and tensor polarizabilities and some hyperpolarizabilities of four even-parity states ($6p^2\ ^3P_2$, $6s7d\ ^3D_{1,2}$, and $5d6d\ ^3D_1$) of Ba lying between 35 600 and 36 000 cm^{-1} (Fig. 1). Three of these four states have polarizabilities more than two orders of magnitude larger than might be expected from the known energy levels of Ba, implying the existence of two as-yet-unidentified close-lying states of odd parity. Looking for Stark-induced excitations of odd-parity states, we identified transitions to the $6s8p\ ^3P_1$ state and to two other states that may be the previously unidentified $6s8p\ ^3P_{0,2}$ states, and measured these states' energies and polarizabilities. The existence of these states explains the unusually large polarizabilities reported here.

Some of the polarizabilities determined in this work are the largest measured for any atomic states with principal quantum number $n<10$, with the exception of the nearly degenerate states of hydrogen. Highly polarizable diatomic molecules [13] and Rydberg atoms [14,15] have been used to measure electric fields, for example, in noncontact circuit board testing. The states of Ba studied here could fulfill the same purpose but with a much broader dynamic range. Highly polarizable levels are also of use in experiments searching for (parity and time-reversal violating) atomic electric-dipole moments [16], although the short lifetimes of the levels studied here may limit their usefulness in this regard. Finally, this work demonstrates the use of Stark-induced transitions for the observation of previously unidentified energy levels, a technique that, to our knowledge, has not been previously used for this purpose.

Pulsed lasers excite Ba atoms in an atomic beam (Fig. 2) to the even-parity states of interest via two successive $E1$ transitions (Fig. 3). Two tunable dye lasers (Quanta Ray PDL-2) pumped by synchronized frequency-doubled Nd-YAG (yttrium aluminum garnet) lasers (Quanta Ray DCR-11 and Quantel YAG580) that produce 10 ns pulses at 10 Hz repetition rate are used. One dye laser, using Fluorescein 548, is tuned to resonance with the 554.7 nm $6s^2\ ^1S_0 \rightarrow 6s6p\ ^1P_1$ transition. The other dye laser, using Rhodamine 6G, is tuned from 556 nm to 570 nm using a combination of diffraction grating angle adjustment and changing nitrogen pressure in the laser cavity. In order to avoid ac Stark shifts of the second-stage transitions, the relative timing of the two laser pulses is offset by ~25 ns. The laser linewidths are ~20 GHz without an intracavity etalon, or ~6 GHz when a narrowing etalon is employed. Color glass filters are used to reduce the pulse energy to ~0.4 mJ to avoid power-broadening effects. In the interaction region the counter-propagating beams are ~3 mm in diameter.

The Ba beam effusion source has a multislit nozzle that collimates angular spread to ~0.1 rad in both the horizontal and vertical directions. The oven is resistively heated to

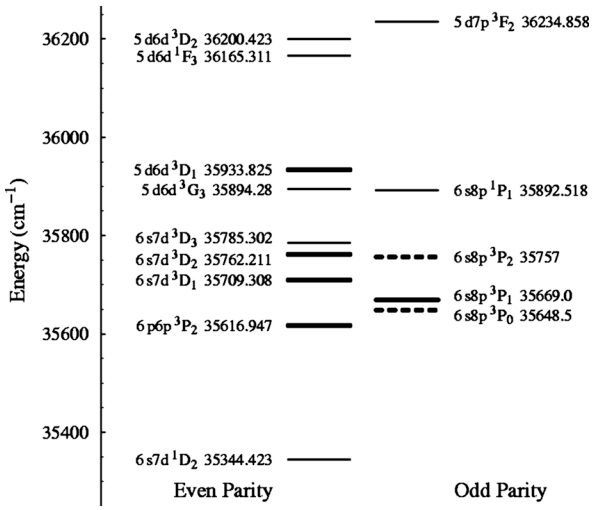

FIG. 1. Partial energy spectrum of Ba. The thicker lines indicate the states whose polarizabilities are measured in this work. The dashed lines denote the previously unidentified energy levels.

*Electronic address: chihhao@socrates.berkeley.edu
†Electronic address: simonkeys@yahoo.com
‡Electronic address: mgk@MF1309.spb.edu
§Electronic address: budker@socrates.berkeley.edu

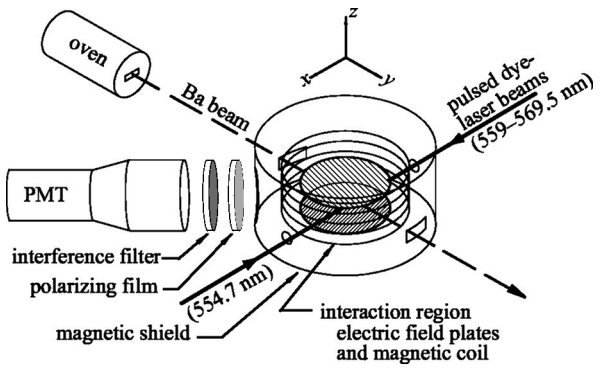

FIG. 2. Simplified schematic diagram of the apparatus.

~700 °C, corresponding to saturated Ba pressure ~0.1 Torr inside the source and estimated atomic beam density $\sim 10^{11}$ atoms per cm^3 in the interaction region, ~20 cm away from the nozzle. Residual gas pressure in the vacuum chamber is $\leqslant 10^{-5}$ Torr.

Fluorescence resulting from spontaneous decay to a lower-lying state is observed with a photomultiplier tube, at 45° to both the atomic and laser beams. Interference filters with 10 nm bandwidth are used to select the decay channel of interest, and a color glass filter is used to further reduce the scattered light from the lasers.

Voltage of up to 80 kV is applied (using a feedthrough described in Ref. [16]) between parallel electrodes of diameter 6.4 cm, spaced 0.9153(3) cm apart, splitting and shifting the resonance signals (Fig. 4) and allowing Stark-induced transitions to neighboring odd-parity states. Individual resonances are identified with particular Zeeman sublevels using their dependence on laser polarization (Table I). Excitation of the $M=0$ sublevel of a $J=1$ state is nominally forbidden in our experimental setup. Resonances corresponding to such excitation are still observed, however, with a signal amplitude one order of magnitude smaller than for the allowed transitions, most likely because of imperfections in the direction and purity of the laser polarizations. The polarizabilities and hyperpolarizabilities are determined from the dependence of the splitting on the electric field (Fig. 5) as we now describe.

The static polarizability α for a state $|a_0 J_0 M\rangle$ with energy $E_{a_0 J_0 M}$ (a_0 represents additional quantum numbers) is defined by

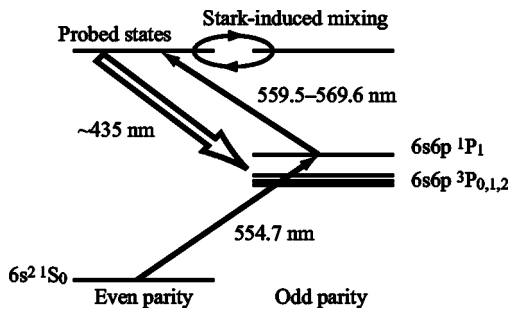

FIG. 3. The excitation-detection scheme. Solid arrows indicate laser excitation; the hollow arrow indicates fluorescence. Odd-parity states are excited due to Stark-induced mixing.

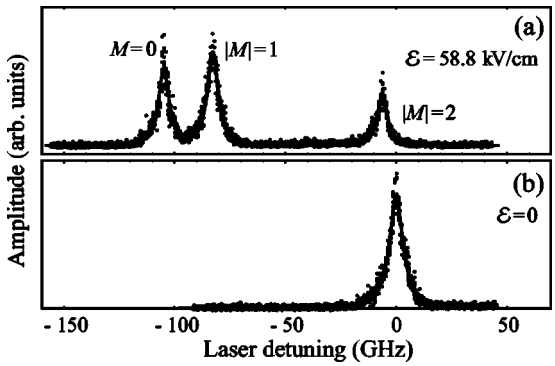

FIG. 4. Fluorescence from the $6p^2\ ^3P_2$ state as a function of laser frequency with (a) an electric field applied and (b) no electric field. The data are fit by Lorentzian functions.

$$\alpha_{a_0 J_0 M} \equiv -2\delta_S E^{(2)}_{a_0 J_0 M} \mathcal{E}^{-2}, \tag{1}$$

where the quadratic Stark shift $\delta_S E^{(2)}_{a_0 J_0 M}$ due to mixing with all other states $|a_1 J_1 M\rangle$ by a weak z-directed field of magnitude $\mathcal{E}$ is given by

$$\delta_S E^{(2)}_{a_0 J_0 M} = \sum_{a_1 J_1} \frac{|\langle a_0 J_0 M | D_z | a_1 J_1 M\rangle|^2 \mathcal{E}^2}{E_{a_0 J_0 M} - E_{a_1 J_1 M}}, \tag{2}$$

where **D** is the electric-dipole operator. In terms of the scalar and tensor polarizabilities α_0 and α_2,

$$\alpha_{a_0 J_0 M} = \alpha_0^{a_0 J_0} + \alpha_2^{a_0 J_0} \frac{3M^2 - J_0(J_0+1)}{J_0(2J_0-1)}. \tag{3}$$

The fourth-order shift $E^{(4)}_{a_0 J_0 M}$, important for stronger mixing, is characterized by the hyperpolarizability

$$\gamma_{a_0 J_0 M} = -4!\ \delta_S E^{(4)}_{a_0 J_0 M} \mathcal{E}^{-4} \tag{4}$$

or, in terms of the scalar and tensor hyperpolarizabilities, γ_0 and $\gamma_{2,4}$ [7],

TABLE I. Zeeman sublevels of states with total angular momentum $J=0,1,2$ that can be excited by two $E1$ transitions involving various combinations of light polarizations [17]. The initial state has $J=0$, the intermediate state has $J=1$.

	Polarizations of laser beams			
J	z,z	y,z or z,y	y,y	$y,z+iy$
0	$M=0$		$M=0$	$M=0$
1		$M=\pm 1$		$M=\pm 1$
2	$M=0$	$M=\pm 1$	$M=0,\pm 2$	$M=0,\pm 1,\pm 2$

$$\gamma_{a_0 J_0 M} = \gamma_0^{a_0 J_0} + \gamma_2^{a_0 J_0} \frac{3M^2 - J_0(J_0+1)}{J_0(2J_0-1)} + \gamma_4^{a_0 J_0} \frac{35M^4 + [25 - 30J_0(J_0+1)]M^2 + (J_0-1)J_0(J_0+1)(J_0+2)}{J_0(2J_0-1)(2J_0-2)(2J_0-3)}. \quad (5)$$

The polarizabilities and hyperpolarizabilities obtained in this work are listed in Tables II and III. The electric-field dependence of the Stark shifts can be used to calculate dipole matrix elements using solutions of the secular equation involving two or more levels. For weak mixing, known values of the energy splittings must be used in order to extract the dipole matrix elements, as can be seen from Eq. (2). For stronger mixing, both the matrix elements and the energy splittings can be extracted from the data (Table IV). The extracted energy splittings can be compared to known splittings to check the validity of neglecting the mixing with other energy levels.

The polarizabilities of three of the even-parity states, $6s7d\ ^3D_1$, $6s7d\ ^3D_2$, and $6p^2\ ^3P_2$, are too large to be due to the known energy spectrum of Ba, suggesting that unidentified odd-parity states with large dipole coupling to these even-parity states lie in this energy region. (The polarizabilities of the fourth even-parity state, $5d6d\ ^3D_1$, agree with our estimates based on the known energy levels.) Measured Stark shifts can be used to extract information about the position and angular momenta of unknown odd-parity states that may be coupled to these even-parity states. For the $6s7d\ ^3D_1$ state, at least one $J=0$ or 2 odd-parity state lying somewhat below this state is required to explain the high polarizability of the $M=0$ sublevel. For the $6s7d\ ^3D_2$ state, the Stark shift of the $M=0$ sublevel can be explained by coupling with the $6s8p\ ^3P_1$ level, whereas the shifts of the $M=\pm1, \pm2$ sublevels cannot (Fig. 6). This indicates that another unknown close-lying odd-parity state, with $J=2$, is responsible for the high polarizabilities of these sublevels. The fact that it apparently does not couple to the $6s7d\ ^3D_1$ state (since it does not strongly cancel the contribution to the Stark shift of this state from the $6s8p\ ^3P_{1,0}$ states) indicates that the unknown state is probably a $^3P_2$ state, mixing with which is subject to suppression because $\Delta J = -\Delta L$ (see Ref. [18], p. 212). Thus it is most likely the unidentified $6s8p\ ^3P_2$ state. We solve the secular equation for a three-level system consisting of the $6s7d\ ^3D_{2,3}$ and the $6s8p\ ^3P_2$ states with three free parameters, namely the electric-dipole moments between the $6s7d\ ^3D_{2,3}$ states and the $6s8p\ ^3P_2$ state and the energy of the $6s8p\ ^3P_2$ state. Using this method to fit the $6s7d\ ^3D_2\ M=\pm2$ Stark-shift data, we determine the energy of the $6s8p\ ^3P_2$ state to be 35 756(1) cm^{-1}. For the $6p^2\ ^3P_2$ state, dipole matrix elements estimated for the coupling of different sublevels to the nearby $6s8p\ ^3P_1$ state are larger than expected, as this is nominally a two-electron transition, but approximately equal (Table IV). This indicates that configuration mixing, rather than coupling to other nearby levels, may be responsible for the high polarizabilities of this state.

To confirm the existence of the two previously unidentified odd-parity states predicted above, we looked for fluorescence from normally forbidden two-photon transitions to odd-parity states that become allowed here due to Stark mixing with even-parity states (Fig. 3). Five resonances were seen in this energy region and identified as transitions to sublevels of three different odd-parity states (Table V). One of these states is the previously observed $6s8p\ ^3P_1$ state [19]. The other two are probably the $6s8p\ ^3P_{0,2}$ states, the only previously unidentified states of Ba that are expected to lie in this energy region. The existence of the $6s8p\ ^3P_{0,2}$ state explains the large polarizability of the $6s7d\ ^3D_{1,2}$ states. Extrapolation of the Stark-induced resonances shows that the zero-field energies (Table V) of the $6s8p\ ^3P_{0,2}$ states are consistent with those predicted above using polarizability data. The extrapolated energy of the $6s8p\ ^3P_2$ state has a large uncertainty because of the lack of low-field data for this state. This determination can be improved by fitting all of the Stark-shift data with the solution of the secular equation

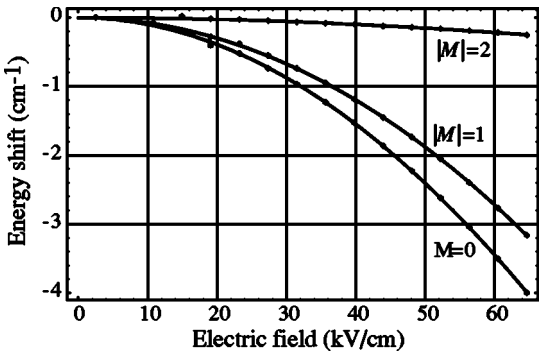

FIG. 5. The Stark splitting and shift of the $6p^2\ ^3P_2$ resonance as a function of electric field. The fit determines the polarizabilities and hyperpolarizabilities given in Tables II and III.

TABLE II. Observed scalar and tensor polarizabilities.

State	α_0 [MHz $(kV/cm)^{-2}$]	α_2
$6p^2\ ^3P_2$	31.05(9)	−27.3(1)
$6s7d\ ^3D_1$	−93(1)	26.6(5)
$6s7d\ ^3D_2$	−335(13)	−268(13)
$5d6d\ ^3D_1$	−4.2(2)	2.0(1)
$6s8p\ ^3P_0$	176(3)	
$6s8p\ ^3P_1$	97(6)	24(3)
$6s8p\ ^3P_2$	$\geqslant$370	$\geqslant$60

TABLE III. Observed scalar and tensor hyperpolarizabilities.

State	γ_0	γ_2 [kHz (kV/cm)$^{-4}$]	γ_4
$6p^2\ ^3P_2$	−2.2(1.6)	0(1)	−0.6(3)
$6s7d\ ^3D_1$	61(3)	−5(2)	

TABLE IV. Experimental reduced electric-dipole matrix elements and level splittings obtained here from Stark-shift data along with known level splittings and matrix elements estimated using the Bates-Damgaard (BD) approximation, neglecting level mixing [18]. Two-level models are used except for the group $6s7d\ ^3D_2$, $6s7d\ ^3D_3$, $6s8p\ ^3P_2$, which is treated as part of a ten-level system.

Observed state		Mixed state	ΔE (cm^{-1}) Expt.	Known	$\|D\|$ (ea_0) Expt.	BD
$6p^2\ ^3P_2$	$M=0$	$6s8p\ ^3P_1$		−52.0(2)	14.7(2)	
$6p^2\ ^3P_2$	$M=\pm1$	$6s8p\ ^3P_1$		−52.0(2)	14.3(2)	
$6s7d\ ^3D_2$	$M=0$	$6s8p\ ^3P_1$	103(20)	93.2(2)	22(2)	34.7
$6s7d\ ^3D_2$	$M=\pm2$	$6s8p\ ^3P_2$	5(1)		16.2(5)	15.5
$6s7d\ ^3D_3$	$M=\pm2$	$6s8p\ ^3P_2$	28(1)		40(2)	44

TABLE V. Extrapolated zero-field energies of states excited via Stark-induced transitions. Predicted energies are extracted from the Stark-shift data (see text), except for the energy of $6s8p\ ^3P_1$, which is from Ref. [19].

Proposed designation	Energy (cm^{-1}) Extrapolated	Predicted
$6s8p\ ^3P_1 M=0,\pm1$	35,668.8(1)	35,669.0(2)
$6s8p\ ^3P_0 M=0$	35,648.5(1)	<35,709
$6s8p\ ^3P_2 M=\pm1,\pm2$	35,758(3)	35,756(1)
	35,757(1)[a]	

[a]With ten-level approximation.

TABLE VI. Reduced electric-dipole moments (in units of ea_0) obtained as described in Ref. [17] from polarizabilities found here.

	$6s8p\ ^3P_0$	$6s8p\ ^3P_1$	$6s8p\ ^3P_2$
$6p^2\ ^3P_2$	0	14.34(6)	6.0(1)
$6s7d\ ^3D_1$	15.9(1)	12.4(2)	
$6s7d\ ^3D_2$	0	21(3)	14(2)
$5d6d\ ^3D_1$	14(2)	⩽15	

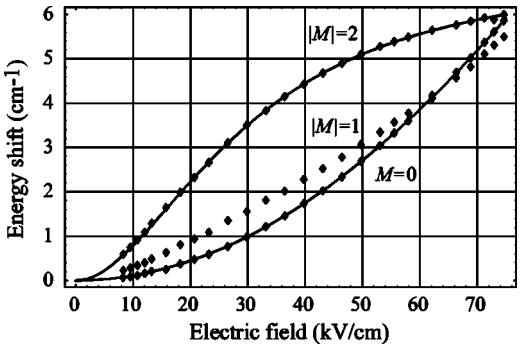

FIG. 6. The Stark splitting and shift of the $6s7d\ ^3D_2$ resonance as a function of electric field. The shifts depend quadratically on the applied field strength only up to a strength of ~10 kV/cm. The shift of the $M=0$ sublevel is described well by a model in which the sublevel interacts with one other level. The $M=\pm2$ sublevel shifts require two other levels in their description. The shifts of the $M=\pm1$ sublevels apparently cannot be described as due to the interaction with a few nearby levels.

written for the ten-level system consisting of all states between 35 600 cm^{-1} and 36 000 cm^{-1} using 15 free parameters, 14 reduced electric-dipole matrix elements and the energy of $6s8p\ ^3P_2$. We determine this energy to be 35 757(1) cm^{-1}, in agreement with the prediction made above.

Alternative determinations of the dipole matrix elements can be made (Table VI) by considering various linear combinations of the scalar and tensor polarizabilities that exclude mixing with levels of specific angular momentum [17]. In this analysis, the *LS*-coupling scheme is used. The configuration and spin-orbit mixing are estimated according to the known energy spectrum.

The quoted errors are primarily due to data fitting uncertainties resulting from the use of models with simplified level structure. The dominant source of experimental systematic error comes from the temporal drift of the Fabry-Perot interferometer used for laser-frequency calibration or, in the case of the study of Stark-induced transitions, of the diffraction grating position. This drift can be tracked using the zero-field positions of the known even-parity atomic resonances as markers. The residual error on the determination of the positions of resonance peaks after accounting for the time dependence of the frequency calibration is ~500 MHz (~6 GHz for the study of the Stark-induced transitions). A secondary source of experimental systematic uncertainty is the 0.03% error in determination of the electric field. Stark shifts of the intermediate $6s6p\ ^1P_1$ state are too small to affect the results. Other sources of systematic error, including the dynamic Stark effect, electronic noise, and the hyperfine structures of the Ba isotopes with nonzero nuclear spin, are found to be negligible.

In conclusion, we have measured the scalar and tensor polarizabilities of four even-parity states of barium in the range of 35 600–36 000 cm^{-1}, and the hyperpolarizabilities

of two of these states. Three of the states have unexpectedly large polarizabilities, suggesting the existence of two previously unidentified states. These two states have been identified by laser spectroscopy on Stark-induced transitions, and polarizabilities have been measured for these states, as well as for a third odd-parity state.

The authors thank V. V. Yashchuk and D. English for experimental help and useful discussions, and B. P. Das, D. P. DeMille, W. Gawlik, M. Kuchiev, and J. E. Stalnaker for helpful advice. This research was supported by NSF Career Grant No. PHY-9733479 and the Miller Institute for Basic Research in Science.

[1] A. Kreutztrager and G. V. Oppen, Z. Phys. A **265**, 421 (1973).
[2] A. Kreutztrager, G. V. Oppen, and W. Wefel, Phys. Lett. **49A**, 241 (1974).
[3] A. Hese, A. Renn, and H. S. Schweda, Opt. Commun. **20**, 385 (1977).
[4] B. Fechner, P. Kulina, and R. H. Rinkleff, Z. Phys. A **307**, 375 (1982).
[5] P. Kulina and R. H. Rinkleff, Z. Phys. A **313**, 241 (1983).
[6] K. A. H. van Leeuwen, W. Hogervorst, and B. H. Post, Phys. Rev. A **28**, 1901 (1983).
[7] P. Kulina and R. H. Rinkleff, Z. Phys. A **318**, 251 (1984).
[8] J. Li and W. A. Van Wijngaarden, in *QELS *95. Summaries of Papers Presented at the Quantum Electronics and Laser Science Conference*, Technical Digest Series Conference Edition Vol. 16 (Optical Society of America, Washington, DC, 1995), pp. 193–4.
[9] B. Schuh, C. Neureiter, H. Jaeger, and L. Windholz, Z. Phys. D: At., Mol. Clusters **37**, 149 (1996).
[10] R. H. Rinkleff and R. Wehmschulte, Z. Phys. D: At., Mol. Clusters **39**, 139 (1997).
[11] D. DeMille, D. Budker, N. Derr, and E. Deveney, Phys. Rev. Lett. **83**, 3978 (1999).
[12] D. English, D. Budker, and D. DeMille, in *Spin-Statistics Connection and Commutation Relations: Experimental Tests and Theoretical Implications*, edited by Robert C. Hilborn and Guglielmo M. Tino, AIP Conf. Proc. No. 545 (AIP, Melville, NY, 2000), p. 281.
[13] M. Auzinsh, R. Ferber, O. Nikolayeva, N. Shafer-Ray, and M. Tamanis, J. Phys. D **34**, 624 (2001).
[14] P. P. Herrmann, J. Hoffnagle, N. Schlumpf, V. L. Telegdi, and A. Weis, J. Phys. B **19**, 1271 (1986).
[15] M. Auzinsh, L. Jayasinghe, L. Oelke, R. Ferber, and N. Shafer-Ray, J. Phys. D **34**, 1933 (2001).
[16] S. M. Rochester, C. J. Bowers, D. Budker, D. DeMille, and M. Zolotorev, Phys. Rev. A **59**, 3480 (1999).
[17] C. Li, S. Rochester, M. Kozlov, and D. Budker, e-print physics/0307060.
[18] I. I. Sobelman, *Atomic Spectra and Radiative Transitions* (Springer, Berlin, 1992).
[19] J. A. Armstrong, J. J. Wynne, and P. Esherick, J. Opt. Soc. Am. **69**, 211 (1979).